Multi-Site Techno-Economic Analysis of Closed-Loop Geothermal Systems

Raquel SP Hakes[1], Radoslav Bozinoski[1], Mohammed (Jabs) Aljubran[2], Gabriela Bran Anleu[1], Anastasia Bernat[3], Alex Buchko[3]

[1]Sandia National Laboratories[*], Livermore, CA, USA

[2]National Renewable Energy Laboratory, Golden, CO, USA

[3]Pacific Northwest National Laboratory, Richard, WA, USA

Keywords

Closed-loop geothermal, advanced geothermal systems, next-generation geothermal, reservoir simulations, techno-economic analysis, convective heat transfer, GeoCLUSTER

ABSTRACT

The Closed Loop Geothermal Working Group (CLGWG) is a multi-lab collaborative consortium, funded by the U.S. Department of Energy Geothermal Technologies Office and focused on the techno-economics of closed loop systems for heating and power generation. The CLGWG has modeled U-loop and co-axial systems considering various technologies (e.g., vacuum-insulated tubing, multilaterals, enhanced near-wellbore thermal conductivity, flexible dispatch) and physical phenomena (e.g., non-steady temperature decline, background convective heat transfer, pressure and heat gain/loss, thermosiphon effect). In this work, we applied these models to 11 selected sites across the United States, classified into three geological categories: basin and range (e.g., Desert Peak, Roosevelt Hot Springs, Coso), volcanic regions (Newberry, Fenton Hill, Imperial Valley), and sedimentary basins (Eagle Ford, Haynesville, New York Appalachian, West Virginia Appalachian, Denver-Julesburg). For each site, we modeled the physical behavior using subsurface characteristics, including ambient temperature, geothermal gradient, target depth, and rock properties (e.g., density, permeability, thermal conductivity, specific heat capacity) for different closed-loop designs. We found significant variability in economic competitiveness across sites, particularly impacted by mass flow rate of the working fluid, drilling cost, and drilling depth. Separately, on-the-fly simulations and convective models were integrated into GeoCLUSTER, an open-source web simulator that enables closed loop developers, investors, and enthusiasts to analyze closed loop designs across different surface and subsurface settings.

---

[*] Sandia National Laboratories is a multimission laboratory managed and operated by National Technology and Engineering Solutions of Sandia, LLC., a wholly owned subsidiary of Honeywell International, Inc., for the U.S. Department of Energy National Nuclear Security Administration under DE-NA0003525. SAND2025-09776C.

1. Introduction

Recently, closed-loop geothermal systems (CLGS), also known as advanced geothermal systems, have received renewed commercial interest. CLGS have some advantages over other geothermal systems, such as conservation of the heat transfer working fluid, thus allowing for different fluids (Beckers et al. 2022). Additionally, they may be attractive in areas where produced water contamination must be avoided, water resources are limited, or stimulation treatments are not available due to regulatory or technical restrictions. At the same time, CLGS face challenges associated with the limited surface area for heat transfer, which requires long wellbores and laterals to obtain multi-MW output (White et al. 2024, Hakes et al. 2024, Aljubran et al. 2024), resulting in high system costs.

In this work, we apply models developed previous in the Closed Loop Geothermal Working Group (CLGWG), a multi-lab collaborative consortium funded by the U.S. Department of Energy Geothermal Technologies Office, to 11 selected sites across the country, to evaluate the techno-economic competitiveness of different closed-loop designs. Additionally, we describe expansions to the GeoCLUSTER application produced by the working group. These include the addition of on-the-fly simulations and a parameter study of convective reservoirs to extend the existing pre-tabulated databases.

In this paper, we present a comprehensive multi-site analysis across basin and range, volcanic, and sedimentary basins. Section 2 presents background on the GeoCLUSTER application produced by the working group. Section 3 describes the selected sites that are investigated. Section 4 presents out research methods and discusses the two simulation codes, Sierra Thermal/Fluids: Aria, a generalized Galerkin finite element method code (Notz et al. 2016), and the slender-body theory (SBT) model (Beckers et al. 2015). The Flexible Geothermal Economics Model (FGEM) (Aljubran and Horne 2024) was then used to evaluate the techno-economic performance of closed loop systems simulated using Aria and SBT. Section 5 provides the updates to the GeoCLUSTER application since it was last presented (Bernat et al. 2025). Section 6 describes the results of the techno-economic site-specific simulations and comparisons between sites. Overall conclusions are provided in Section 7.

2. GeoCLUSTER Background

GeoCLUSTER V2.0 (url: https://geocluster.labworks.org/) is an open-source, techno-economic web simulator for CLGS that provides primary users like venture capitalists or start-up developers with a collection of interactive methods for streamlining the exploration of the economic viability of CLGS via computationally fast modeling and high-quality datasets. The application was created using Python for its computations and Dash as its web framework. The tool requires Python 3.8-3.12 because Python 3.13 is not supported due to CoolProp incompatibility; likewise, it requires Dash >=2.9.2, which supports advanced callbacks. The entire cloud-based platform operates on an Amazon EC2 instance, and its deployment process from its GitHub repository (https://github.com/pnnl/GeoCLUSTER) to the EC2 instance is automated through the integration of GitHub and AWS Code Deploy. Furthermore, GeoCLUSTER is deployed on an Apache web server configured with Web Server Gateway Interface (WSGI) acting as a reverse proxy to enable secure, scalable, and production-ready deployments by bridging the app with the web server and managing HTTP traffic efficiently. To navigate GeoCLUSTER, users can query, generate, and visualize CLGS in conduction-only reservoirs via a large but compressed, precomputed HDF5

dataset of over 2.5 million simulation runs (see White et al. 2024 for details). Notably, a recent data engineering solution that chunks the HDF5 dataset reduced the application's memory footprint by 97% (i.e., from 6.5 GB to 200 MB) (Bernat, et al. 2025). This chunking solution divides the 8D simulation dataset into smaller subsets (chunks), and, at runtime, only loads the chunks surrounding a user's input parameters to perform 8D linear interpolation, enabling efficient and memory-light data retrieval.

Additionally, with recent updates, users can run on-the-fly simulations of their CLGS computed by the SBT model for approximating heat production and profiling pressure over time. Notably, a recent sparse matrix solution ensures that CPU usage remains below 4%. This sparse matrix solution uses compressed sparse column (CSC) matrices – an efficient format that stores only non-zero values and their locations – to solve large systems of linear equations at each simulation time step. These equations arise from modeling heat transfer and fluid flow; solving them with a sparse-aware linear solver (e.g., spsolve) significantly reduces both memory usage and computation time. In turn, despite GeoCLUSTER offering real-time simulations that are normally computationally intensive, its low CPU usage enables scalability for multiple users, reduces cloud computing costs, and supports deployments on low-resource environments like burstable EC2 instances.

Finally, all V1.0 visuals are retained, including charts displaying subsurface and economic results linearly over time, contour representations between a parameter and mass flow rate, and summary tables of parameter values and their results. However, in V2.0, users have access to an additional 10 new parameters to edit, supporting a total of 31 editable parameters, when users select to simulate with SBT. The full editable parameter list of GeoCLUSTER V2.0 can be referenced on its GitHub page.

3. Site Selections

A total of 11 sites were selected for simulation and techno-economic evaluation. These sites are qualitatively classified into three categories: basin and range, volcanic regions, and sedimentary basins. We chose sites with available data that are geographically representative and inclusive of various geothermal and oil and gas fields. We surveyed the literature to collect subsurface properties at commonly drilled depths for each site, including geothermal gradient, depth, in-situ rock properties (thermal conductivity, specific heat capacity, density, and permeability). Sites are shown in Table 1 with subsurface properties shown in Tables 3 and 4. In cases where reported subsurface properties were inconsistent for a given site, we investigated further and elected those references listed first for each site to be most accurate.

Table 1: Category and location of selected sites. References indicate the source of subsurface properties.

Category	Site	References
Basin and Range	Desert Peak, Nevada	Kraal et al. (2021); Blankenship et al. (2016); Smith et al. (2023)
Basin and Range	Roosevelt Hot Springs, Utah	Moore et al. (2022); Gwynn et al. (2019)
Basin and Range	Coso, California	Blankenship et al. (2016); Sabin et al. (2016)
Volcanic Regions	Newberry, Oregon	Bonneville et al. (2016); Frone et al. (2014)

Volcanic Regions	Fenton Hill, New Mexico	Duchane et al. (2002); Kelkar et al. (2016); Norbeck et al. (2018)
Volcanic Regions	Imperial Valley, California	Barkman et al. (1976); Sass et al. (1984); Mase et al. (1981)
Sedimentary Basins	Eagle Ford Shale, Texas	Hou et al. (2022); Abdi (2014); Tian et al. (2013)
Sedimentary Basins	Haynesville Shale, Louisiana	Hou et al. (2022); Brittenham (2013)
Sedimentary Basins	Appalachian, New York	Fulton (2024); Beckers et al. (2024)
Sedimentary Basins	Appalachian, West Virginia	Garapati et al. (2020); Zhang et al. (2020)
Sedimentary Basins	Denver-Julesburg (D-J) Basin, Colorado	Higley et al. (2005); Davalos-Elizondo et al. (2024)

4. Simulation Methods

Simulations of convective reservoirs were conducted in Sierra Thermal/Fluids: Aria (version 5.24), a generalized Galerkin finite element method code (Notz et al. 2016) to add convective reservoirs to the existing database of pre-tabulated results in GeoCLUSTER. Conduction-only reservoir simulations were conducted using both Aria and the SBT model (Beckers et al. 2015) for site-specific simulations. Techno-economic analysis was performed using FGEM, which uses the output temperatures calculated by either Aria or the SBT model. The simulations for these two thrusts had differing parameters kept constant or changing to allow for exploring specific phenomena of interest (e.g., the convection parameter study varied permeability across a wide range of values to see where convection onset, but kept conductivity constant, whereas the site-specific simulations used a constant prescribed conductivity associated with the specific reservoir).

4.1 Aria Methods

The Aria simulations explore heat extraction through a full L-shaped coaxial or U-tube loop geometry. Conductive simulations are run using the model described in White et al. 2024. Convective simulations are run using the model and equations described in Bran Anleu et al. 2025. Domain dimensions for both hot wet rock and hot dry rock are chosen such that there are negligible edge effects. In both conductive and convective simulations, the vertical and horizontal sections of the domain are decoupled from each other except through the 1D heat exchanger, which runs the full length of the domain. The 1D heat exchanger assumes heat transfer through the radius of the working fluid and the thickness of the pipe are negligible, given that the length of the heat exchanger (several km) substantially exceeds its diameter (<1 m).

For convective simulations, the vertical well is modeled as hot dry rock (conduction-only), while the lateral section is hot wet rock (conduction and convection) made of permeable layers. The impermeable domain is 2D axisymmetric with a radius of 150 m. The permeable domain is 3D: the length of the lateral and 250 m in the other two coordinate directions. For convective simulations, higher permeability rock is sandwiched between an overburden and underburden of lower permeability rock (consistent with Hakes et al. 2024). The mass and heat flow in the hot wet rock are modeled as single-phase Darcy flow with the formation fluid modeled as pure liquid water. With sufficient thermal gradient and permeability (see Hakes et al. 2024, Bran Anleu et al. 2025 for required permeabilities of minimum 100 mD to see convective effects), the variation of

fluid density with temperature due to the heat exchanger can give rise to buoyantly driven convection currents, drawing warmer water to the heat exchanger and allowing cooled water to pool below the heat exchanger. The domain is initially at hydrostatic pressure, and the initial formation temperature is set according to the depth and geothermal gradient (specific parameters described for the different applications below). The vertical sides are impervious to heat and mass flow and can be considered symmetry planes. The top and bottom surfaces are maintained at the initial temperatures.

4.1.1 Aria Parameters for GeoCLUSTER Convection Simulations

The impact of natural convection in both a U-loop and an L-shaped coaxial system was considered for varying parameters of the working fluid, reservoir, and system characteristics (see Table 2). Parameter ranges for the convection study are more limited than the current HDF5 database, due to the increased computational intensity of convective simulations. Borehole diameter is kept constant at 0.4445 m for GeoCLUSTER simulations. While large, this diameter is consistent with the upper values currently in GeoCLUSTER, and impacts of varied parameters are anticipated to be apparent regardless of diameter. Values for rock conductivity, specific heat capacity, and density are kept constant between simulations at 3.05 W/m-K., 790 J/kg-K, and 2750 kg/m^3, respectively. Working fluid is assumed to be pure water for all simulations presented.

Table 2: Variation of parameters for convective simulations added to GeoCLUSTER.

Parameter	Values
Mass flow rate (kg/s)	2, 10
Drilling depth (m)	1, 5
Horizontal extent (m)	1, 2.5, 5
Geothermal gradient (°C/km)	30, 60
Injection temperature (°C)	30, 60
Permeability (mD)	100, 500, 1000

4.1.2 Aria Methods for Site Specific Simulations

For the 11 selected sites, we considered both U-tube and L-shaped coaxial systems in hot dry rock at a depth relevant to the reservoir (see Table 3) and with horizontal laterals of 1000, 2500, and 5000 m. The working fluid is assumed to be pure water in all simulations, with an injection temperature of 60°C and a borehole diameter of 0.2445 m (9.625 in). Reservoir and rock characteristics used for the simulations are presented in Table 3 Table 4. In cases where surface temperature was not reported, it was estimated based on the reported subsurface temperature, average geothermal gradient, and true vertical depth. While we see a wide range of permeabilities (porous and fractured rocks are more permeable than non-fractured basement rocks), we assume conductive heat transfer only for these simulations, as the permeabilities are below what was found to cause convective flow in previous studies (Hakes et al. 2024, Bran Anleu et al. 2025); thus, permeability is provided for information about the reservoir, but not used in the simulations. The focus for these simulations is on CLGS in these locations, so we do not consider the impact of fracture, which is of greater interest for other geothermal systems.

Table 3: Site specific reservoir characteristics. Reservoir temperature indicates the target temperature but is not prescribed in simulations. Rather, reservoir temperature at every location is a function of the surface temperature, geothermal gradient, and depth.

Site/Region	Geothermal Gradient [C/km]	Drilling Depth [m]	Surface Temperature [°C]	Reservoir Temperature [°C]
Desert Peak	76	2750	20	229
Roosevelt Hot Springs	70	2600	40	222
Coso	74	2500	66	251
Newberry	100	3000	15	315
Fenton Hill	65	4000	20	280
Imperial Valley	130	2000	25	285
Eagle Ford Shale	40	4000	25	185
Haynesville Shale	37	5000	25	210
Appalachian	23	3000	15	84
Appalachian	32	5000	15	175
D-J Basin	50	3000	15	165

Table 4: Prescribed bulk reservoir rock properties for the selected sites. All properties are assumed to be constant throughout the reservoir. Permeability is a uniform matrix permeability and provided for informational purposes, but not prescribed in conductive simulations.

Site/Region	Conductivity [W/mK]	Specific heat capacity [J/kgK]	Density [kg/m^3]	Bulk permeability [mD]
Desert Peak	1.95	700	2400	0.1
Roosevelt Hot Springs	3.05	790	2750	0.048
Coso	2.2	800	2660	0.1
Newberry	2.3	850	2670	2.6
Fenton Hill	2.4	800	2650	0.0001
Imperial Valley	2	850	2500	20
Eagle Ford Shale	1.6	850	2500	0.01
Haynesville Shale	1.6	850	2500	0.001
Appalachian (CUBO)	2.7	850	2800	0.1
Appalachian (UWV)	2.7	900	2800	0.1
D-J Basin	2.9	800	2650	100

4.2 SBT Methods

Originally developed by Beckers et al. (2015), SBT is a semi-analytical framework for modeling conductive heat transfer in CLGS where the length of the heat exchanger substantially exceeds its diameter, a common characteristic of CLGS configurations. This approach streamlines the simulation of transient conductive heat transfer between the circulating fluid and the surrounding rock formation by treating the wellbore as a series of line sources rather than a fully discretized three-dimensional domain. The CLGS wellbore heat exchanger is discretized into multiple segments, each considered as a finite-length heat source embedded within a uniform, homogeneous geological medium. The model then leverages Green's function solutions to the transient heat conduction equation to compute the time-dependent temperature response of the rock matrix to each heat source segment. By applying the superposition principle, SBT captures the cumulative thermal interaction between all segments along the wellbore trajectory, allowing it to account for both near-wellbore heat transfer and long-term reservoir cooling effects.

SBT is a semi-analytical model, hence it is computationally efficient (see Beckers et al. 2015 for details, as relative computational efficiency varies from one model to another), enabling rapid evaluation of different scenarios across a broad range of operating conditions and system configurations. This efficiency is especially advantageous when conducting parametric studies or fully coupling the model with transient lifecycle techno-economic frameworks such as FGEM. Additionally, recent extensions of the SBT model have enhanced its applicability to more complex scenarios, including systems with variable flow rates, multi-lateral well designs, and dynamic operational strategies (Beckers et al. 2022; Aljubran et al. 2025). These developments continue to establish SBT as a key modeling tool for CLGS analysis, bridging the gap between detailed numerical simulations and high-level techno-economic evaluations.

This study leveraged SBT as integrated into FGEM by Aljubran et al. (2024) to evaluate the techno-economic performance of vertical co-axial systems for power generation in terms of the levelized cost of electricity (LCOE). Whereas Table 3 indicates depths typically targeted across the respective sites, drilling deeper is advantageous to avail greater resource temperatures. In this analysis, we targeted a reasonable true vertical depth of 7 km across sites. The average geothermal gradients and rock thermal conductivity reported in Tables Table 3Table 4 cannot be used to characterize these resources at a depth of 7 km. Instead, we used temperature-at-depth and in-situ rock thermal conductivity predictions based on the Stanford thermal Earth modeling approach developed by Aljubran and Horne (2024b,c). Figure 1 shows temperature profiles across the selected sites down to depths of 10 km.

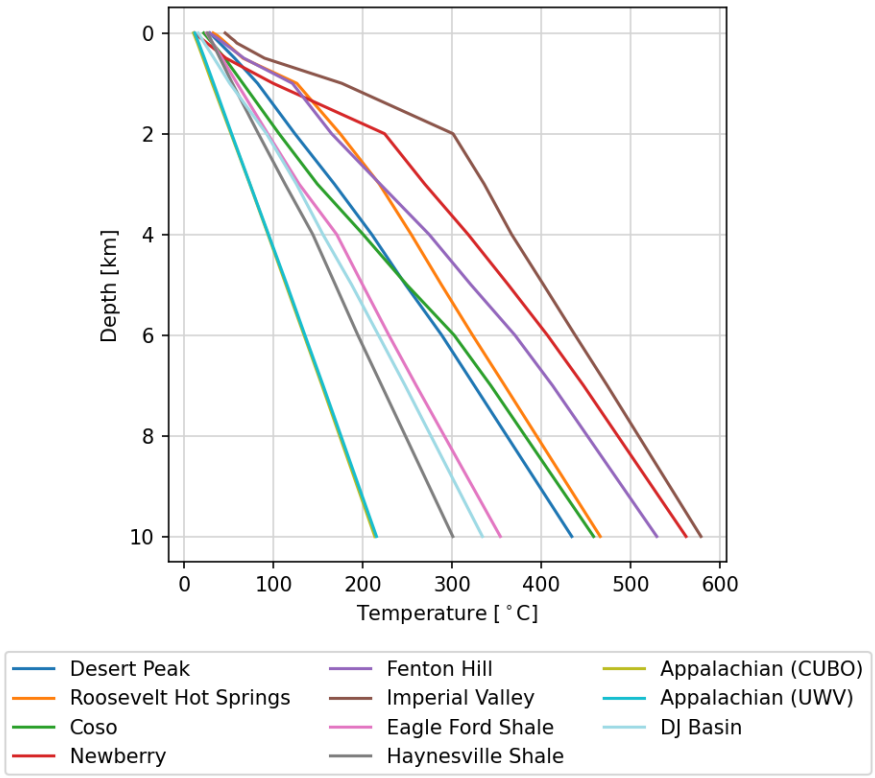

Figure 1: Temperature profile across the selected sites, based on the Stanford thermal model.

Each site was developed with ten co-axial wells drilled to a true vertical depth of 10 km, each completed with a 0.2445 m (9.625 inch), 40 lbs/ft production casing and equipped with 0.088 W/m-°C vacuum-insulated tubing, based on a design reported by Chen et al. (2024). These design choices aim at evaluating the techno-economics for a hypothetical project involving a power plant, rather than a single well. We considered different flow rates (i.e., 2, 4, 6, 8, and 10 kg/s) per well to find more optimal LCOE across sites. An air-cooled Organic Rankine Cycle (ORC) power plant (Aljubran and Horne 2025) was used, with an iterative scheme to search the optimal on-design hot-side temperature depending on the corresponding site conditions (i.e., production and ambient temperatures). A low drilling cost of 500 USD/meter was considered alongside power plant cost of ~2300 USD/kWe across sites. We choose a low drilling cost to evaluate whether the improvement of drilling cost, simultaneous with targeting deeper formations, yields more economic co-axial systems. Aljubran et al. 2024a provides details on the correlations FGEM uses to estimate these costs. Discount rate was set to 7% for a project lifetime of 40 years.

5. GeoCLUSTER Updates

The GeoCLUSTER application developed by the CLGWG has been expanded to

1) include on-the-fly simulations using an SBT model, and
2) pre-tabulated results for convective reservoirs.

5.1 SBT Solver Optimization

To integrate the SBT model, we profiled the run time of the SBT code. At a high level, the SBT models work by constructing a linear equation that simulates a CLGS and then solving it. We found that the majority of the runtime was consumed by the solving of this linear equation (approximately 95% solving and 5% setup). We also found that the matrices involved in the equation were sparse, that is mostly composed of zeros. By changing the data type we used from the default NumPy array to the CSC matrix, which is optimized for sparse matrices, and by changing our linear algebra solver to one that was also optimized for sparse matrices (spsolve), we were able to reduce the run time by approximately 20% (approximately 24 sec of run time, saving 7-10 sec per simulation).

5.2 Convective Simulation Additions

The convection dataset is similar to the previous Bernat et al. (2025) simulation dataset in that at each parameter combination, it describes the output of the CLGS over time. For GeoCLUSTER's purposes, the output of a CLGS is the output temperature, pressure, electric power, and thermal power. We can model each of these outputs and the relation to their inputs by constructing a response surface: a 7-dimensional NumPy array where each point in the array represents the output at a given input parameter combination (see White et al. 2024 for validation studies). The 7 dimensions include the six independent parameters seen in Table 5 as well as time, with each simulation modeling a 40-year cycle. Similar to the previous version of GeoCLUSTER, we can use linear interpolation on this response surface to estimate the output of a CLGS at parameter combinations whose values fall in between the simulated parameter combinations. These response surfaces, as well as their input values, were saved to an HDF5 file as shown in Table 5. They are all saved as NumPy arrays with the input parameters being 1-dimensional and the output datasets being 7-dimensional.

Table 5: Description of Convection Dataset Modified for GeoCLUSTER.

Parameter Name	Location in HDF5	Shape of NumPy Array
Mass flow rate	/input/mdot	(2)
Drilling depth	/input/depth	(3)
Horizontal extent	/input/horizontal_extent	(3)
Geothermal gradient	/input/grad	(2)
Injection temperature	/input/t_inj	(2)
Permeability	/input/perm_HWR	(3)
Time	/input/time	(241)
Output pressure	/output/Pout	(2, 3, 3, 2, 2, 3, 241)
Output temperature	/output/Tout	
Output electric power	/output/kWe	
Output thermal power	/output/kWt	

5.2.1 Computational Requirements

Because the parameter space of the convection dataset is relatively small, the additional computational needs for GeoCLUSTER to include it are minimal. It takes a fraction of a second to interpolate or fetch the values from a response surface, and since each matrix contains only (2

* 3 *3 * 2 *2 *3 * 241) = 52,056 64-bit floats, each matrix only requires approximately 25KB of RAM to hold in memory. With four matrices needed, GeoCLUSTER only requires an additional 0.1MB of RAM. Additionally, because the dataset is small compared to the previous dataset, the chunking strategy mentioned in Bernat et al. (2025) has not been needed so far. Instead, all four matrices are held entirely in memory.

6. Site-specific Techno-economic Results

Figure 2 shows the output temperature results for the simulations of U-loop and L-shaped coaxial at target depths for the selected sites. Only the 5000 m results are shown; however, trends were similar for 1000 m and 2500 m laterals with lower steady state production temperatures as the lateral length decreased. Here, we see that many sites, at the depths and system parameters chosen, do not produce sufficiently higher temperatures to likely be viable. Note that Eagle Ford Shale and Fenton Hill are not shown here. Due to issues surrounding our computational infrastructure, we were unable to complete desired coaxial runs for these sites. However, runs in the U-tube configuration with a 5000 m lateral found steady state production temperatures of approximately 85°C and 140°C for Eagle Ford Shale and Fenton Hill, respectively, solidly within the range of other results shown. As a result, we assume that coaxial results would be similarly within range.

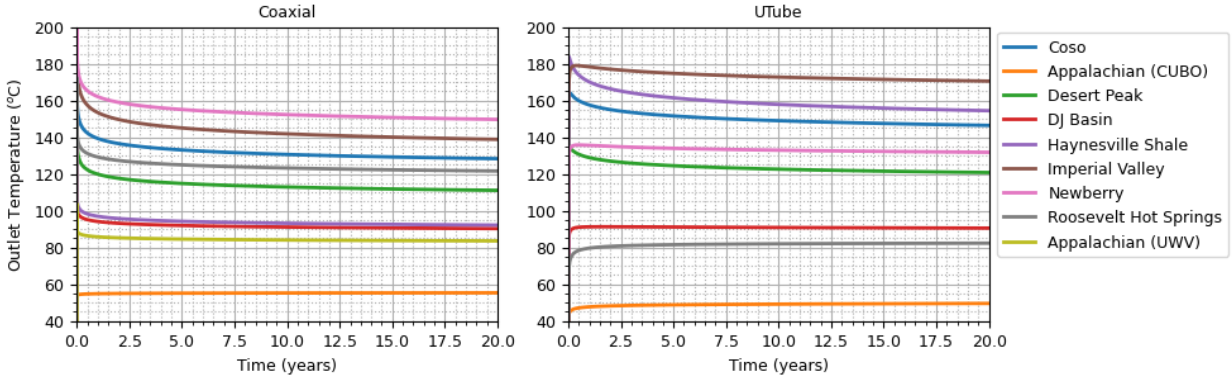

Figure 2: Production temperature as a function of time for (left) an L-shaped coaxial configuration with target reservoir depth and a 5000 m lateral and (right) a U-tube configuration at target depth with a 5000 m lateral.

Given that many sites experienced production temperatures below 150°C, we focused out initial techno-economic analysis on a single site to explore economic viability. For the initial analysis, we considered the Newberry site with an L-shaped coxial configuration and a 5000 m lateral. To do this, we coupled Aria with FGEM to analyze the lifecycle assuming 10 wells behaving as the single well presented in Figure 2. This model was configured as seen in **Error! Reference source not found.**.

Table 6: Techno-economic input parameters used to evaluate the lifecycle performance at the Newberry site.

Surface and Subsurface Characteristics			
Geothermal gradient	100°C/km	Vertical depth	3 km
Surface temperature	15°C	Bottomhole temperature	440°C
Ambient temperature	Seasonally variable	Rock thermal conductivity	2.3 W/m-°C
System Design and Operations			

Power plant type	air-cooled ORC	Installed nameplate capacity	5 MWe
Plant on-design temperature	157°C	Number of wells	10
Mass flow rate per well	10 l/s fresh water	Casing outer/inner diameter	9.625/8.835 inch
Economic Parameters			
Project lifetime	40 years	Discount factor	7%
Drilling cost	500 USD/meter	Power plant cost	2,386 USD/kWe
Contingency	0%	O&M cost	132 USD/kWe-year

We assumed favorable drilling costs of 500 USD/meter (Akindipe and Witter 2025). Ambient temperature was configured as an annually repeating series of historical temperature records for a default site in the United States, as shown in Figure 3. The system resulted in an LCOE of 109 USD/MWhe and generated a total of 36.9 GWhe electricity annually (i.e., 3.69 GWhe per well). Capital expenditure was 48.3 million USD, with drilling and power plant costs representing 72% and 28%, respectively. Operational expenditure was 132 USD/kWe-year, with wellsite and power plant costs representing 48% and 52%, respectively. Water loss is negligible in co-axial CLGS. Akindipe and Witter (2025) reported that standard drilling rates for similar well designs were nearly 2,800 USD/meter, which would yield an LCOE of 389 USD/MWhe.

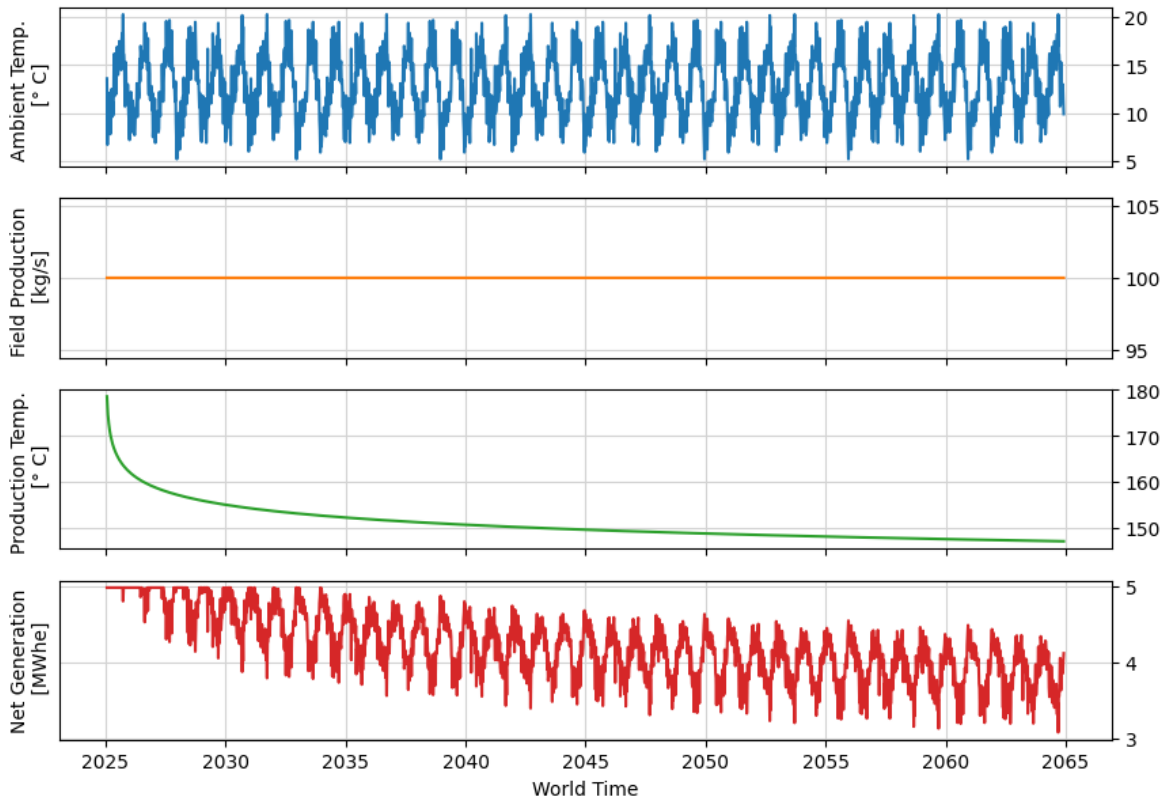

Figure 3: Major input and output parameters of an L-shaped co-axial systems at the Newberry site, simulated by coupling Aria with FGEM.

The production temperature experiences a specific temporal behavior, starting in transient period, early in time, with a sharp drop, followed by a slower decline. CLGWG investigated a variety of CLGS and determined that these decline temperature characteristics are common across designs and stem from conduction through reservoir rock as the dominant heat transfer mechanism in CLGS. The sharp early decline in production temperature has significant implications to the CLGS economic viability (Bernat et al., 2025; White et al., 2024) and justifies the considerably high LCOE of 389 USD/MWhe estimated in this study under standard drilling rates. Net generation started at the installed nameplate capacity of 5 MWe during the first ~10 years when outlet fluid temperature is sufficiently high, before dropping to around 3.75 MWe. Seasonal oscillations were observed as the power plant was governed by changes in ambient temperature, where high summer ambient temperatures cause power output reductions to nearly 3.1 MWe during the last few years of operation.

Given the low production temperatures for most sites at the target depth, we explored options to increase the viability of the sites: by varying the mass flow rate of the working fluid and drilling deeper. To account for realistic drilling strategies and achievable future drilling costs (developing L-shaped co-axial systems at great depth is challenging), we focused subsequent analysis on vertical coaxial systems with VIT. All sites have a similar system configuration to Table 6, but with a true vertical depth of 10 km. We used the Stanford thermal Earth model to evaluate temperature and in-situ rock thermal conductivity at these depths, seen in Figure 1. Again, we assumed favorable drilling costs of 500 USD/meter (Akindipe and Witter 2025). For each site, we accounted for subsurface uncertainty using a Monte Carlo approach, where we sampled temperature-at-depth and in-situ rock thermal conductivity from the distribution predicted by the Stanford thermal Earth model. For each sample, we evaluated system performance under a range of flow rates (i.e., 2, 4, 6, 8, and 10 kg/s) and selected the flow rate design that yielded minimal LCOE for the respective site. Table 7 shows the optimal flow rate for each site used in the subsequent LCOE estimates, as well as other relevant site-specific parameters.

Table 7: Techno-economic input parameters and basic outputs for each site. Note that these LCOE values assume a highly optimistic drilling rate of 500 USD/m and wells of 10 km true vertical depth.

Site	Mass Flow Rate [kg/s]	Bottomhole Temperature [°C]	Rock Thermal Conductivity [W/m-C]	Installed Nameplate Capacity [MWe]	LCOE [USD/MWhe]
Desert Peak	4	434	2.11	3.67	152.82
Roosevelt Hot Springs	6	466	2.38	6.18	120.10
Coso	6	459	2.36	6.00	123.25
Newberry	6	562	2.29	7.97	96.38
Fenton Hill	6	529	2.88	7.41	89.00
Imperial Valley	6	579	2.05	8.24	96.36
Eagle Ford shale	4	354	2.41	2.22	215.30
Haynesville Shale	4	301	1.87	1.36	475.66

Appalachian	4	215	2.40	0.08	52125.50
D-J Basin (Basement)	4	334	2.48	1.87	262.86

As seen in Figure 4, we evaluated LCOE across sites and quantified uncertainty accordingly. This figure was truncated at 600 USD/MWhe for visual convenience. We note that three sites yielded average near-optimal LCOE of <100 USD/MWhe, namely Newberry, Fenton Hill, and Imperial Valley. These sites belong to the "Volcanic Regions" category, seen in Table 1. Given the elevated geothermal gradients, the cost-competitive LCOEs are anticipated. Note this techno-economic analysis assumed an optimistic drilling rate of 500 USD/m.

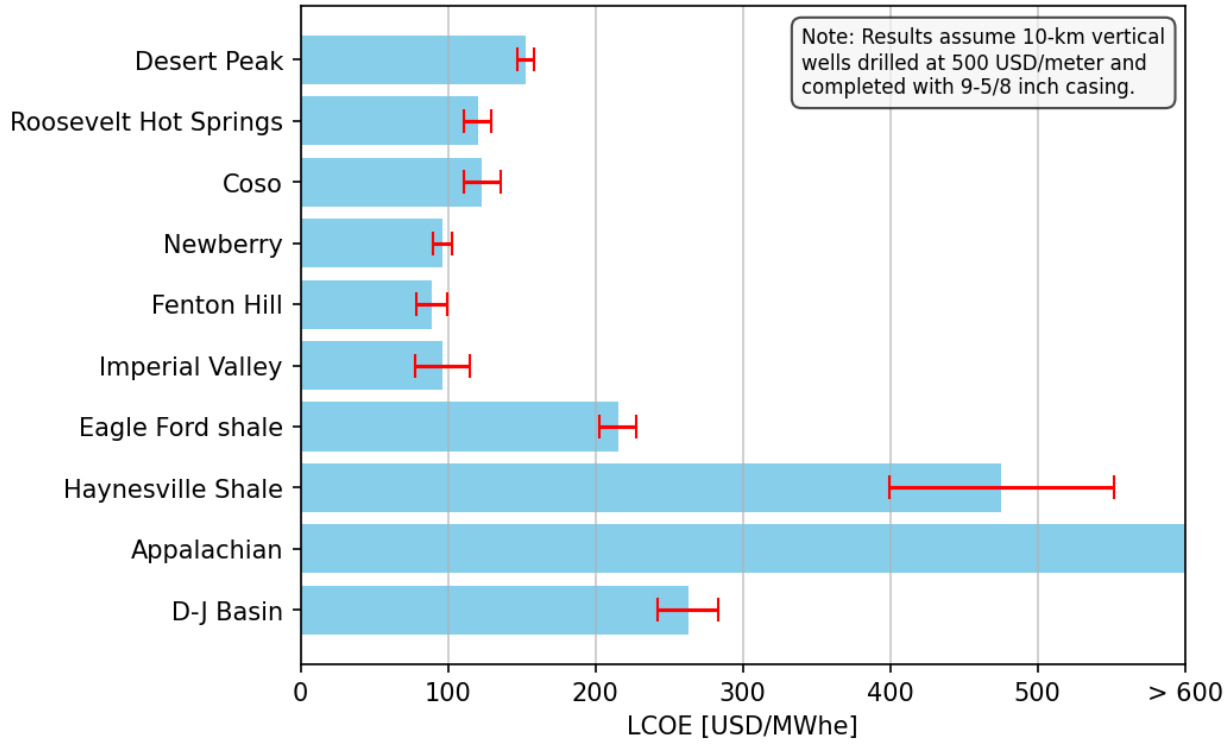

Figure 4: LCOE across selected sites, with error bar indicating techno-economic uncertainty stemming from subsurface uncertainty predicted by the Stanford thermal Earth model. Note that this techno-economic analysis assumed optimistic drilling rates of 500 USD/meter.

7. Conclusions

In this paper, we present the results of a multi-site techno-economic analysis, as well as updates from the CLGWG, which include several GeoCLUSTER updates that expand the simulation space considered. Techno-economic analysis found that sites needed a minimum viable output temperature to produce viable economic results, often requiring lower mass flow rates. Additionally, sites were most viable with lower than industry-average drilling rates, indicating the need to continue pursuing decreased cost of drilling. Comparing sites at typically drilled depths with targeting deeper areas indicated the potential advantages of drilling deeper; however, these advantages again require an overall decrease in drilling cost.

Acknowledgement

Funding provided by the U.S. Department of Energy Office of Energy Efficiency and Renewable Energy Geothermal Technologies Office. This work was authored in part by the National Renewable Energy Laboratory, operated by Alliance for Sustainable Energy, LLC, for the U.S. Department of Energy (DOE) under Contract No. DE-AC36-08GO28308, and in part by the Pacific Northwest National Laboratory, operated by Battelle Memorial Institute, for the U.S. Department of Energy (DOE) under contract GT0100000-05450-1005612 (2022). This paper describes objective technical results and analysis. Any subjective views or opinions that might be expressed in this paper do not necessarily represent the views of the U.S. Department of Energy or the United States Government. The U.S. Government retains and the publisher, by accepting the article for publication, acknowledges that the U.S. Government retains a nonexclusive, paid-up, irrevocable, worldwide license to publish or reproduce the published form of this work, or allow others to do so, for U.S. Government purposes.

REFERENCES

Abdi, Z. (2014). Chemostratigraphy of the Austin Chalk and Upper Eagle Ford Shale, south central, TX. The University of Texas at Arlington.

Aljubran, M.J, Beckers, K., Mibei, G., and Horne, R.N. “Techno-Economic Viability of Flexible Dispatch of Unconventional Geothermal Systems.” *GRC Transactions*, Vol. 49 (2025).

Aljubran, M. J., and Horne, R.N. "FGEM: Flexible Geothermal Economics Modeling tool." Applied Energy 353 (2024a): 122125.

Aljubran, M.J., and Horne, R.N. “Thermal Earth Model for the Conterminous United States Using an Interpolative Physics-Informed Graph Neural Network.” *Geothermal Energy*, 12(1), 25. (2024b).

Aljubran, M. J., and Horne, R. N. “Power Supply Characterization of Baseload and Flexible Enhanced Geothermal Systems.” Scientific reports, 14(1), 17619. (2024c)

Barkman, J. H., Campbell, D. A., Smith, J. L., & Rex, R. W. (1976). East Mesa--Geology, Reservoir Properties and an Approach to Reserve Determination (No. SGP-TR-20-17). Republic Geothermal, Inc., Santa Fe Springs, CA.

Beckers, K.F., Koch, D.L. and Tester, J.W. “Slender-Body Theory for Transient Heat Conduction: Theoretical Basis, Numerical Implementation and Case Studies.” Proceedings of the Royal Society A: Mathematical, Physical and Engineering Sciences, 471(2184), p.20150494. (2015).

Beckers, K. F., Rangel-Jurado, N., Chandrasekar, H., Hawkins, A. J., Fulton, P. M., & Tester, J. W. “Techno-economic Performance of Closed-loop Geothermal Systems for Heat Production and Electricity Generation.” Geothermics, 100, 102318. (2022).

Beckers, K., Hawkins, A., Erdinc, B., & Tester, J. (2024). EGS Reservoir Modeling for Developing Geothermal District Heating at Cornell University (No. NREL/CP-5700-90305). National Renewable Energy Laboratory (NREL), Golden, CO (United States).

Bernat, A., Buchko, A., Beckers, K., Moreno, A. (2025) GeoCLUSTER v2.0: A Closed-Loop, Techno-Economic Simulator Supporting New Case Studies. In: PROCEEDINGS 50th Workshop on Geothermal Reservoir Engineering, Stanford University, Stanford, CA.

Blankenship, D. A., Akerley, J., Blake, K., Calvin, W., Faulds, J. E., Glen, J., et al. (2016). Frontier Observatory for Research in Geothermal Energy: Phase 1 Topical Report Fallon, NV (No. SAND2016-8929). Sandia National Lab.(SNL-NM), Albuquerque, NM (United States).

Blankenship, D. A., Blake, K., Calvin, W., DeOreo, S., Faulds, J. E., Glen, J., ... & Williams, C. (2016). Frontier Observatory for Research in Geothermal Energy: Phase 1 Topical Report West Flank of Coso, CA (No. SAND2016-8930). Sandia National Lab.(SNL-NM), Albuquerque, NM (United States).

Bonneville, A., Cladouhos, T. T., & Schultz, A. (2016, February). Establishing the Frontier Observatory for Research in Geothermal Energy (FORGE) on the Newberry Volcano, Oregon. In PROCEEDINGS, 41st Workshop on Geothermal Reservoir Engineering Stanford University, Stanford, California.

Bran Anleu, G., Hakes, R.S.P., Bozinoski, R., Beckers, K. (2025) A Parametric Study of L-Shape Coaxial Closed-Loop Geothermal Systems with Reservoir Convection. In: PROCEEDINGS 50th Workshop on Geothermal Reservoir Engineering, Stanford University, Stanford, CA.

Brittenham, M. D. (2013). Geologic analysis of the upper Jurassic Haynesville shale in East Texas and West Louisiana: discussion. Aapg Bulletin, 97(3), 525-528.

Chen, G., Wright, C., Liu, J., Gomez, C., and Garcia, A. "Modeling a Deep Coaxial Closed-Loop Vacuum Insulated Tubing (VIT) Completion in a Geothermal Research Test Well Using FEFLOW." Proceedings: ARMA US Rock Mechanics/Geomechanics Symposium. (2024).

Davalos-Elizondo, E., Taverna, N., Gold, A., Menon, K., & Trainor-Guitton, W. (2024). Geothermal Play Fairway Analysis of Low-Temperature Resources for Sedimentary Basin Geothermal Play Types: An Example in the Denver Basin (No. NREL/TP-5700-91108). National Renewable Energy Laboratory (NREL), Golden, CO (United States).

Duchane, D., & Brown, D. (2002). Hot dry rock (HDR) geothermal energy research and development at Fenton Hill, New Mexico. Geo-Heat Centre Quarterly Bulletin, 23.

Frone, Z., Waibel, A., & Blackwell, D. (2014, February). Thermal Modeling and EGS Potential of Newberry Volcano, Central Oregon. In Proceedings, Thirty-Ninth Workshop on Geothermal Reservoir Engineering at Stanford University.

Fulton, P., Clairmont, R., Fulcher, S., Pinilla, D., Purwamaska, I., Jamison, H., et al. (2024). Subsurface Insights from the Cornell University Borehole Observatory (CUBO): A 3km Deep Exploratory Well for Advancing Earth Source Heat Deep Direct-Use Geothermal for District Heating. In Proceedings of the 49th Workshop on Geothermal Reservoir Engineering, Stanford, CA, USA (pp. 12-14).

Garapati, N., Irr, V. J., & Lamb, B. (2020). In Feasibility Analysis of Deep Direct-Use Geothermal on the West Virginia University Campus-Morgantown, WV. In Proceedings, 45th Workshop on Geothermal Reservoir Engineering, Stanford University, Stanford, CA.

Gwynn, M., Allis, R., Hardwick, C., Jones, C., Nielsen, P., & Hurlbut, W. (2019). Compilation of rock properties from FORGE well 58-32, Milford, Utah. Geothermal Characteristics of the

Roosevelt Hot Springs System and Adjacent FORGE EGS Site, Milford, Utah: Utah Geological Survey Miscellaneous Publication, 169.

Hakes, R.S.P., Bozinoski, R., Beckers, K.F., Ketchum, A. (2024) Influence of Reservoir Convection on Heat Extraction with Closed-Loop Geothermal Systems. *GRC Transactions*, Vol. 48.

Higley, D. K., & Cox, D. O. (2005). Oil and gas exploration and development along the front range in the Denver Basin of Colorado, Nebraska, and Wyoming. US Geological Survey professional paper, (1698), 13-53.

Hou, L., Cui, J., & Zhang, Y. (2022). Evolution mechanism of dynamic thermal parameters of shale. Marine and Petroleum Geology, 138, 105423.

Kelkar, S., Wolde Gabriel, G., & Rehfeldt, K. (2016). Lessons learned from the pioneering hot dry rock project at Fenton Hill, USA. Geothermics, 63, 5-14.

Kraal, K. O., Ayling, B. F., Blake, K., Hackett, L., Perdana, T. S. P., & Stacey, R. (2021). Linkages between hydrothermal alteration, natural fractures, and permeability: Integration of borehole data for reservoir characterization at the Fallon FORGE EGS site, Nevada, USA. Geothermics, 89, 101946.

Mase, C. W., Sass, J. H., Brook, C. A., & Munroe, R. J. (1981). Shallow hydrothermal regime of the East Brawley and Glamis known geothermal resource areas, Salton Trough, California (No. 81-834). US Geological Survey,.

Moore, J., Pankow, K., McLennan, J., Podgorney, R., Finnila, A., Erickson, B., Feigl, K., Batzli, S., Nash, G., Skowron, G., Wannamaker, P., Jones, C., Simmons, S., Hardwick, C., Kirby, S., Doe, T., Damjanac, B., Xing, P., Radakovic-Guzina, Z., Deo, M., Munday, L., Bolisetti, C., & Wilkins, A. (2022). Utah FORGE: Phase 3A, Year 2, Annual Report. [Data set]. Geothermal Data Repository. Energy and Geoscience Institute at the University of Utah. https://gdr.openei.org/submissions/1401

Norbeck, J. H., McClure, M. W., & Horne, R. N. (2018). Field observations at the Fenton Hill enhanced geothermal system test site support mixed-mechanism stimulation. Geothermics, 74, 135-149.

Notz, P.K., et al. (2016) SIERRA Multimechanics Module: Aria User Manual. Tech. rep. Albuquerque, NM: Sandia National Laboratories.

Sabin, A., Blake, K., Lazaro, M., Meade, D., Blankenship, D., Kennedy, M. et al. (2016). Geologic setting of the West Flank, a FORGE site adjacent to the Coso geothermal field. In Proceedings of the 41st Workshop on Geothermal Reservoir Engineering, Stanford University, Stanford, CA, USA (pp. 22-24).

Sass, J. H., Galanis Jr, S. P., Lachenbruch, A. H., Marshall, B. V., & Munroe, R. J. (1984). Temperature, thermal conductivity, heat flow, and radiogenic heat production from unconsolidated sediments of the Imperial Valley, California (No. 84-490). US Geological Survey,.

Smith, T., Sonnenthal, E., Nakata, N., Cladouhos, T., & Swyer, M. (2023). A Thermal, Hydrological and Mechanical Model of Patua Geothermal Field, Nevada. In Proceedings, 48th

Workshop on Geothermal Reservoir Engineering, Stanford University, Stanford, California, February (pp. 6-8).

White, M., Vasyliv, Y., Beckers, K., Martinez, M., Balestra, P., Parisi, P., Augustine, C., Bran-Anleu, G., Horne, R., Pauley, L., Bettin, G., Marshall, T., & Bernat, A. (2024) Numerical investigations of closed-loop geothermal systems in deep geothermal reservoirs. Geothermics, 116, 102852.

Tian, Y., Ayers, W. B., & McCain Jr, W. D. (2013, March). The Eagle Ford Shale play, South Texas: Regional variations in fluid types, hydrocarbon production and reservoir properties. In International Petroleum Technology Conference (pp. IPTC-16808). IPTC.

Zhang, Y., Garapati, N., Doughty, C., & Jeanne, P. (2020). Modeling study of deep direct use geothermal on the West Virginia university campus-morgantown, WV. Geothermics, 87, 101848.